The Journal of Physiology

T-type amino acid transporter TAT1 (Slc16a10) is essential for extracellular aromatic amino acid homeostasis control

Luca Mariotta[1], Tamara Ramadan[1], Dustin Singer[1], Adriano Guetg[1], Brigitte Herzog[1], Claudia Stoeger[2], Manuel Palacín[3], Tony Lahoutte[4], Simone M. R. Camargo[1] and François Verrey[1]

[1] *Institute of Physiology and Zürich Center for Integrative Human Physiology (ZIHP), University of Zürich, Switzerland*
[2] *Ingenium Pharmaceuticals AG, Martinsried, Germany*
[3] *Institute for Research in Biomedicine (IRB Barcelona), Barcelona, Spain*
[4] *In Vivo Cellular and Molecular Imaging Laboratory, Vrije Universiteit Brussel, Brussels, Belgium*

Key points

- The amino acid (AA) transporter TAT1 (Slc16A10) mediates facilitated diffusion of aromatic AAs (AAAs) across membranes.
- TAT1 null mice lack liver control of AAAs and display altered epithelial AA transport.
- The data support the hypothesis that equilibrative transport of essential AAs by TAT1 is crucial for body AA homeostasis control.

Abstract The uniporter TAT1 (Slc16a10) mediates the facilitated diffusion of aromatic amino acids (AAAs) across basolateral membranes of kidney, small intestine and liver epithelial cells, and across the plasma membrane of non-epithelial cells like skeletal myocytes. Its role for body AA homeostasis has now been investigated using newly generated TAT1 (Slc16a10) defective mice (*tat1*$^{-/-}$). These mice grow and reproduce normally, show no gross phenotype and no obvious neurological defect. Histological analysis did not reveal abnormalities and there is no compensatory change in any tested AA transporter mRNA. TAT1 null mice, however, display increased plasma, muscle and kidney AAA concentration under both normal and high protein diet, although this concentration remains normal in the liver. A major aromatic aminoaciduria and a smaller urinary loss of all substrates additionally transported by L-type AA antiporter Lat2–4F2hc (Slc7a8) were revealed under a high protein diet. This suggests an epithelial transport defect as also shown by the accumulation of intravenously injected ^{123}I-2-I-L-Phe in kidney and L-[^{3}H]Phe in *ex vivo* everted gut sac enterocytes. Taken together, these data indicate that the uniporter TAT1 is required to equilibrate the concentration of AAAs across specific membranes. For instance, it enables hepatocytes to function as a sink that controls the extracellular AAAs concentration. Additionally, it facilitates the release of AAAs across the basolateral membrane of small intestine and proximal kidney tubule epithelial cells, thereby allowing the efflux of other neutral AAs presumably via Lat2–4F2hc.

(Received 10 July 2012; accepted after revision 5 October 2012; first published online 8 October 2012)
Corresponding author F. Verrey: Institute of Physiology, University of Zurich, Winterthurerstrasse 190, CH-8057 Zurich, Switzerland. Email: verrey@access.uzh.ch

Abbreviations AA, amino acid; AAA, aromatic amino acid; BCAA, branched-chain amino acid; CT, computed tomography; PCR, polymerase chain reaction; *wt*, wild-type.

DOI: 10.1113/jphysiol.2012.239574

Introduction

Dietary and endogenous proteins are hydrolysed in the gastrointestinal lumen to tri-peptides, di-peptides and individual amino acids (AAs) that are taken up by small intestine enterocytes (Nassl *et al.* 2011). These cells hydrolyse the oligopeptides into single AAs and also further metabolize some of them. Finally, they release most AAs into the portal circulation, thereby strongly influencing the rate of AA appearance in plasma (Cynober, 2002; Wu, 2009). It is noteworthy that the amount of free AAs transported daily from the enterocytes into the circulation is much larger than the free AA pool of the plasma and extracellular space (∼100 g per day *versus* less than 10 g), such that their uptake into tissues is crucial for maintaining extracellular AA homeostasis (Cynober, 2002). In the cells of different organs, AAs may then serve as building blocks for the synthesis of structural and functional proteins, may be used for cellular metabolism or function as signalling molecules (Verrey *et al.* 2009; Wu, 2009). Therefore, AA transfer across plasma membranes via various cooperating AA transporters plays a crucial role for body AA homeostasis, and the defect of transporters leads to several diseases (Verrey *et al.* 2009; Broer & Palacin, 2011).

The best characterized basolateral AA transporters of the small intestine and proximal kidney tubule (re)absorbing epithelia are the abundant Lat2–4F2hc (Slc7a8) and y^+Lat1–4F2hc (Slc7a7) that function as obligatory exchangers (antiporters). Thus, they do not mediate net AA transport, but are suggested to perform the directional transport of all their substrate AAs in exchange for AAs that can be recycled across the membrane by parallel transporters able to mediate a directional flux (Pfeiffer *et al.* 1999; Rossier *et al.* 1999; Meier *et al.* 2002; Fernandez *et al.* 2003; Verrey, 2003; Verrey *et al.* 2009). The role of Lat2–4F2hc has been recently investigated *in vivo* using a *lat2* defective mouse (Braun *et al.* 2011). Its phenotype was mild, presenting an increase in several small neutral AAs in serum and a corresponding minor aminoaciduria. Based on these published data we estimate that the observed small urinary AA loss of *lat2* null mice is not due to a decreased fractional excretion of AAs, and therefore surprisingly does not point to a substantial epithelial AA transport defect (Braun *et al.* 2011). Interestingly, aromatic AAs (AAAs) were not elevated in the serum of *lat2* null mice, suggesting that another AA transporter plays a dominant role here, possibly the T-type AAA transporter TAT1 (Slc16a10), which was found slightly upregulated in the kidney of *lat2* null animals. This transporter was molecularly identified and first characterized in 2001 by Endou and co-workers (Kim *et al.* 2001). In a later study, we have demonstrated using the *Xenopus laevis* oocyte expression system that TAT1 functions as a facilitated diffusion pathway that mediates the transport of AAAs L-Phe, L-Trp and L-Tyr with symmetric low apparent affinities, for instance with a $K_{0.5}$ of approximately 30 mM for L-Phe influx and efflux (Ramadan *et al.* 2006). Interestingly, TAT1 protein was shown to co-localize in the kidney proximal tubule with the two exchangers mentioned above (Ramadan *et al.* 2007), and also to localize to the basolateral membrane of small intestine enterocytes and the sinusoidal membrane of perivenous hepatocytes (Ramadan *et al.* 2006). The analysis of *tat1* mRNA expression by real-time polymerase chain reaction (PCR) revealed its presence in the epithelial tissues mentioned above, and also in muscles and brain (Ramadan *et al.* 2006). Finally, it was demonstrated that AAAs effluxing via TAT1 can be recycled into the cell by the exchanger Lat2–4F2hc and thereby drive the efflux of other intracellular neutral AAs that are substrates of Lat2–4F2hc (Ramadan *et al.* 2007). To investigate the role that TAT1 plays in whole-body AA homeostasis maintenance and in epithelial AA transport, we generated a TAT1 knockout ($tat1^{-/-}$) mouse and present here its first characterization.

Methods

The *tat1* knockout mouse model was produced by Ingenium Pharmaceuticals AG (Germany) using ENU (*N*-ethyl-*N*-nitrosurea) mutagenesis (Augustin *et al.* 2005; Keays *et al.* 2007). The nonsense mutation in the *tat1* gene leads to a premature stop at position 88 (Y88*). The mice were backcrossed 10 times in a C57Bl/6J inbred strain (Charles River, Germany), which was the background of the parental female, whereas the mutagenized sperm was C3HeBFeJ. All animals were housed in standard conditions in normal light cycle and fed a standard diet prior to experiment. All procedures for mouse handling were according to the Swiss Animal Welfare laws and approved by the Kantonales Veterinäramt Zürich.

Immunofluorescence and real-time PCR

The anti-mTAT1 antibody used has been previously characterized (Ramadan *et al.* 2006), and tissues were processed as described elsewhere (Rossier *et al.* 1999). mRNA was extracted and quantified as described before (Ramadan *et al.* 2006), with the only difference that the reference gene used was HPRT (hypoxanthine guanine phosphoribosyl transferase).

RotaRod test

Mice were put on a rotating drum with an accelerating (day 1, 6–60 r.p.m.) or fixed speed (day 2, average speed reached on day 1; Ugo Basile, model 47600, Italy; Sugiura *et al.* 2005). The time at which the animal

drops off the drum was measured (maximal testing time: 300 s). Five trials were performed on each day. The average value from four different experimental days was calculated.

Different protein diets and metabolic cage experiments

Ten-week-old *tat1*$^{-/-}$ and wild-type (*wt*) littermate mice were fed sequentially with a normal protein diet (20% casein) followed by 8 days of high protein diet (40% casein). The modified standard diet AIN93G was maintained isocaloric by adjusting the starch content (Kliba-Nafg, Switzerland). Chow was put as pellet directly in the normal cages or reduced to powder for the metabolic cage experiment. Mice were weighed daily, and every third day put into metabolic cages (Tecniplast, Buguggiate, Italy) from 08.30 to 16.30 h to adapt, and 24 h (08.30–08.30 h) at the end of each diet period. At the end of the 24 h, urine and faeces were collected, and food and water consumption recorded. Urinary pH was measured using a pH microelectrode (691 pH-meter, Metrohm). Urinary creatinine was measured by the Jaffe method (Seaton & Ali, 1984). Urinary and plasma urea were measured using the diacetyl monoxime method (Wybenga *et al.* 1971). Urinary electrolytes (Na^+, K^+, Ca^{2+}, Mg^{2+}, Cl^-, $SO_4{}^{2-}$) were measured by ion chromatography (Metrohm ion chromatograph, Switzerland). Blood was collected through a single tail tip cut into Na^+-heparinized micro-haematocrit-tubes (Provet AG, Switzerland) and plasma collected after centrifugation at 6000 *g* at 4°C. Animals were anaesthetized with Isoflurane (Provet AG) and killed by decapitation. After death, organs were harvested, frozen in liquid nitrogen and stored at −80°C. For AA measurements, organs were lysed using MagNa Lyser Green Beads (Roche, Switzerland) in PBS supplemented with 1 μl ml^{-1} Protease Inhibitor Cocktail (Sigma, Switzerland), in a ratio of wet weight to PBS volume of 1:3. Supernatant was collected after two 15,000 *g* centrifugations for 15 min at 4°C.

AA measurement

The analysis was done by the Functional Genomics Center Zurich (FGCZ). Samples were deproteinized with 10% sulphosalicylic acid, and AA concentrations were determined using the MassTrak Amino Acid Analysis Solution (Waters, Milford, USA) according to the manufacturer's instructions. The *tat1*$^{-/-}$ plasma AA ratios represented in Fig. 3*B* were normalized to the *wt* ones that were measured within the same diet and that are directly depicted in Fig. 3*A*. The same procedure was used to obtain the normalized urinary values depicted in Fig. 5*B*.

Micro-SPECT/computed tomography (CT) imaging and biodistribution analysis

Imaging and biodistribution of the AAA analogue ^{123}I-2-I-L-Phe was performed in *wt* and *tat*$^{-/-}$ mice. ^{123}I-2-I-L-Phe was synthesized as described before (Bauwens *et al.* 2007). Animals injected with ^{123}I-2-I-L-Phe were anaesthetized and imaged 30 min after intravenous injection with a micro-SPECT (e.cam 180; Siemens, Brussels, Belgium) and a micro-CT (Skyscan 1178; Skyscan, Belgium) system as described before (Lahoutte *et al.* 2002, 2003, 2004; Bauwens *et al.* 2007; Vanhove *et al.* 2011). Images were visualized with the AMIDE 0.9.1 software, where micro-CT is represented in grey scale and micro-SPECT in NIH colour scale (Loening & Gambhir, 2003). After imaging, animals were killed and dissected. All major organs and tissues were collected and counted in a gamma camera counter (Canberra, Belgium) and expressed as percentage of injected activity per gram of organ or tissue.

Everted gut sacs

Uptake on the first two-thirds of the proximal small intestine segments of radiolabelled L-Phe and D-Mannitol was performed as described elsewhere (Nassl *et al.* 2011). Shortly, everted gut sacs were incubated for 10 min at 37°C in bubbling (95% oxygen and 5% carbon dioxide) Krebs-Tris buffer (pH 7.4) containing 100 μM L-Phe, 0.5 μCi L-[^{3}H]Phe/ml (Hartmann Analytic, Germany), 0.02 μCi ^{14}C-D-mannitol/ml (ARC, USA). After brief washing, sacs were cut open and content activity counted (serosa). Sacs were further dried at 55°C O/N on cellulose (Sartorius AG, Germany) and weighed. The sacs (tissue) were lysed in Solvable (Perkin Elmer, Switzerland) for 6 h at 50°C, bleached with 200 μl of 30% H_2O_2, and the radioactivity was determined by liquid scintillation in 15 ml of Ultima Gold (Perkin Elmer). AA transport was expressed relative to the dry tissue weight.

Statistics

Statistical analysis was performed using GraphPad Prism 5.0 (GraphPad Software, USA) and R 2.14 (R Foundation of Statistical Computing). Unless mentioned otherwise, between-group comparisons were performed by Student's unpaired *t* test or by repeated-measures one-way ANOVA, followed by Bonferroni *post hoc* test. Statistical significance was accepted at $P < 0.05$ or as indicated. Data are presented as means ± SEM.

Results

A *tat1* knockout mouse (*tat1*$^{-/-}$) was produced by ENU mutagenesis (Ingenium Pharmaceuticals AG) in

the context of the former European EUGINDAT project. The nonsense mutation (Y88*) was confirmed by DNA sequencing, and the mice were backcrossed 10 times into C57Bl/6J background. Absence of *tat1* expression was confirmed using immunofluorescence and mRNA analysis. The TAT1 protein was indeed not detected in any of the knockout samples tested (Fig. 1*B* and *D*), and the *tat1* mRNA levels were decreased in all tested tissues, but in white adipose tissue (see online Supplemental Table 1a and b, *tat1*), presumably due to nonsense mediated decay (Maquat, 1995).

Mild phenotype under normal conditions

tat1$^{-/-}$ pups grew normally and showed no visible phenotype when compared with their *wt* littermates (online Supplemental Fig. 1). Once adult, *tat1*$^{-/-}$ mice showed no body weight difference compared with *wt* (Table 1), they were fertile and gave birth to normal litters matching the expected Mendelian distribution (data not shown). AAAs transported by TAT1 such as L-Trp and L-Tyr are known to be precursors of serotonin, catecholamines and thyroid hormone. Thus, the absence of TAT1 transporter could potentially impact on neurotransmitter and thyroid hormone availability, and lead to neurological disorders. Although no gross behavioural change was observed, the motor activity and coordination skills of the mice were tested using a RotaRod test (Karl *et al.* 2003), which, however, showed no difference between *tat1*$^{-/-}$ and *wt* littermates (Fig. 2). In an attempt to exacerbate a potential phenotype, the same experiment was carried out after subjecting the mice to a low protein diet (7% casein) for 5 days, without revealing any difference between the two groups (data not shown). In order to visualize a potential abnormal behaviour of *tat1*$^{-/-}$ mice, the animals were video recorded in their normal cage prior and after fasting (data not shown), and their feeding and drinking behaviour recorded for 24 h in metabolic cages (Table 1; Supplemental Table 2). Again, no difference was observed between *tat1*$^{-/-}$ mice and their *wt* littermates, except for a slight increase in water intake and urinary volume that was larger than expected from the increased aminoaciduria (see below). A histological analysis of kidney, liver and intestinal segments on haematoxylin eosin-stained sections also did not reveal any abnormality (Supplemental Fig. 2). A possible upregulation of other AA transporters was then investigated as compensatory mechanisms for TAT1 absence, but no significant change was noticed at the level of any tested AA transporter mRNA in various different organs (Supplemental Table 1a and b) nor at the level of B^0AT1, TMEM27 and Lat2 proteins tested in kidney (data not shown). Also the carbohydrate metabolism did not appear to be perturbed, as indicated

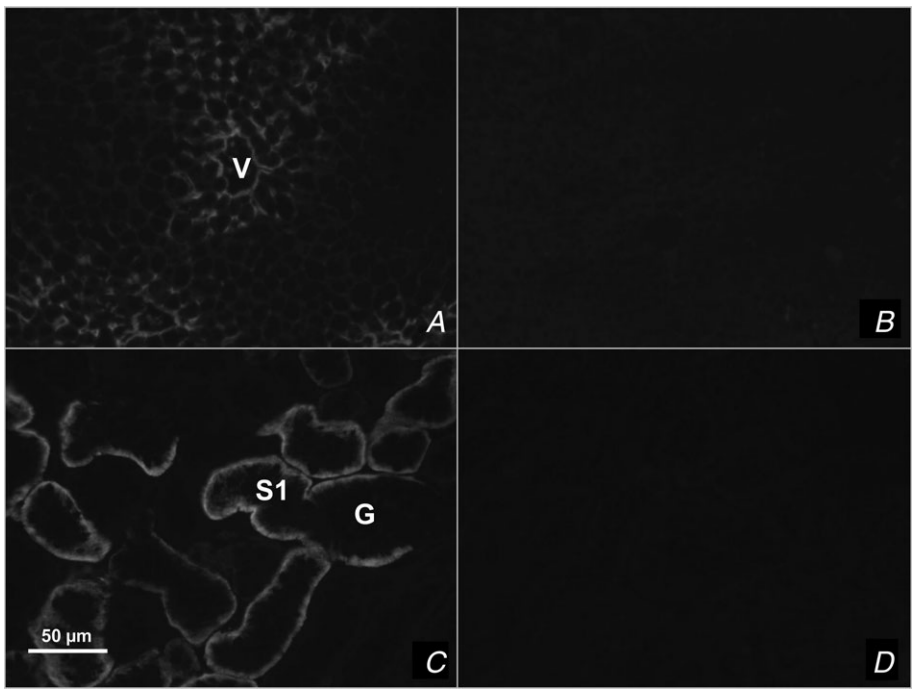

Figure 1. TAT1 detection by immunofluorescence microscopy in sections of liver (*A* and *B*) and kidney (*C* and *D*)
TAT1 is localized to the perivenous hepatocytes (*A*) and kidney proximal tubule cells (*B*) of *wt* tissues, whereas it is not detected in *tat1*$^{-/-}$ tissues (*B* and *D*). G, glomerulus; S1, proximal convoluted tubule segment S1; V, central vein.

Table 1. Urinary and physiological parameters of males measured in metabolic cages for 24 h

	Normal protein diet (20% casein)		High protein diet (40% casein)	
Males	*wt*	*tat1*$^{-/-}$	*wt*	*tat1*$^{-/-}$
Urinary parameters:				
pH	6.36* ± 0.03	6.46 ± 0.07	6.05 ± 0.06 c†	6.11 ± 0.02 d
Creatinine (mg per 24 h)	0.174 ± 0.036	0.510 ± 0.088	1.150 ± 0.299 c	1.898 ± 0.316 d
Creatinine (mg dl^{-1})	40.2 ± 2.6	32.1 ± 2.9	22.8 ± 5.9 c	17.8 ± 0.9
Urea (mg dl^{-1})/crea (mg dl^{-1})	166.7 ± 53.4	133.9 ± 23.4	332.1 ± 32.9 c	277.6 ± 29.5 d
Na^+ (mM)/crea (mg dl^{-1})	8.58 ± 0.57	7.90 ± 0.49	9.45 ± 1.22	7.18 ± 0.98
K^+ (mM)/crea (mg dl^{-1})	7.27 ± 0.26	6.38 ± 0.34	6.88 ± 0.71	5.38 ± 0.62
Ca^{2+} (mM)/crea (mg dl^{-1})	0.041 ± 0.001	0.048 ± 0.009	0.089 ± 0.008 c	0.078 ± 0.009
Mg^{2+} (mM)/crea (mg dl^{-1})	0.52 ± 0.06	0.36 ± 0.05	0.70 ± 0.13	0.59 ± 0.10
Osmolality (mosmol (kg H_2O) $^{-1}$)	3148 ± 174	2260 ± 192	2660 ± 497	2072 ± 199
Urine volume (ml (g BW)$^{-1}$)	0.046 ± 0.005	0.086 ± 0.009	0.112 ± 0.019 c	0.164 ± 0.013 d
Water intake (ml (g BW)$^{-1}$)	0.131 ± 0.014	0.244 ± 0.028 a	0.272 ± 0.023 c	0.362 ± 0.021 d
Food intake (g (g BW)$^{-1}$)	0.142 ± 0.013	0.165 ± 0.010	0.144 ± 0.009	0.153 ± 0.009
Faeces (g (g BW)$^{-1}$)	0.021 ± 0.002	0.023 ± 0.001	0.020 ± 0.002	0.019 ± 0.002
Body weight (g)	28.1 ± 1.0	25.7 ± 0.3	27.6 ± 0.8	26.2 ± 0.6
Body weight (% change)	1.00 ± 0.00	1.00 ± 0.00	0.99 ± 0.01	1.02 ± 0.02

*Given are means ± SEM ($n = 6$). †Groups were compared by one-way ANOVA, followed by Bonferroni *post hoc* test on selected pairs of columns. Values with letters are statistically different ($P < 0.05$): 'a' indicates that *tat1*$^{-/-}$ and *wt* are significantly different under normal protein diet, 'c' that *wt* under normal and high protein diet are different and 'd' that *tat1*$^{-/-}$ under normal *versus* high protein diet are different. No sex difference was observed. Female data can be found in Supplemental Table 2.

by a normal oral glucose tolerance test (Supplemental Fig. 3).

Altered homeostasis of AAAs

To assess the general impact of TAT1 absence on AA homeostasis, we measured the plasma concentration of proteinogenic AAs. Surprisingly, the AAA plasma concentration of *tat1*$^{-/-}$ mice was 2, 3 and 7.5 times higher than in *wt* for L-Phe, L-Trp and L-Tyr, respectively (Fig. 3*B*). In contrast, many other AAs were significantly diminished in *tat1*$^{-/-}$ plasma (i.e. Gly, L-Ala, L-Met, L-Ser, L-Thr, L-Asn, L-Gln, L-Lys and L-Arg). In view of the mild general phenotype observed under normal protein diet (20%), the animals were challenged for 8 days with a high protein diet (chow containing 40% of casein). This treatment did not significantly affect their body weight and, besides the expected high urea and creatinine excretion and the lower urinary pH, only an increased fluid intake and urinary volume were observed that can be explained by the increased urea excretion (Table 1; Supplemental Table 2). Indeed, the urea concentration in the urine amounted to ∼1350 mmol l^{-1} under normal diet and ∼1600 mmol l^{-1} under high protein diet. *tat1*$^{-/-}$ mice displayed similar values as their *wt* littermates with a more pronounced effect on fluid intake. Upon a switch to high protein diet, the plasma AAs remained stable in *wt* animals, with the exception of the branched-chain AAs (BCAAs) that increased (Fig. 3*A*). In *tat1*$^{-/-}$ mice, the diet had a similar effect as in *wt* mice, and maintained the peculiar pattern observed under normal diet: an elevated concentration of AAAs and a low concentration of all other AAs, except the BCAAs, which followed the dietary effect observed in the *wt* (Fig. 3*B*).

To further investigate the cause of the AA imbalance, free cytosolic AAs were measured in organs that represent the major reservoirs and metabolic sites: kidney, liver

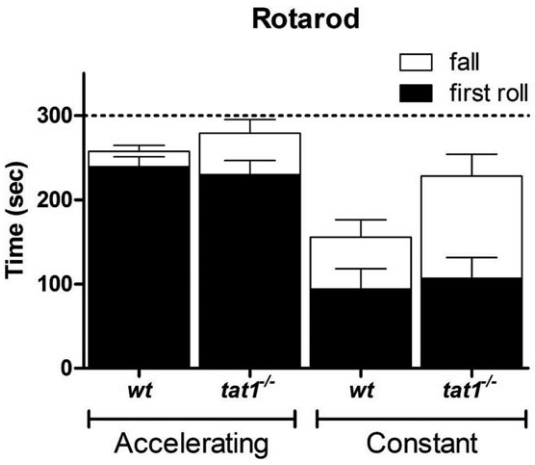

Figure 2. Locomotor and coordination capability of *tat1*$^{-/-}$ and *wt* littermates
Mice were tested with a RotaRod assay at accelerating and constant speed. Represented is the latency time before the first roll occurs (filled bars) and until first fall (open bars). Given are means ± SEM ($n = 5$).

and skeletal muscles. The cellular concentrations of five representative AAs are depicted in Fig. 4. The AAAs L-Tyr and L-Trp displayed values strictly parallel to plasma in kidney and skeletal muscle. In contrast, in liver AAAs remained at the same lower concentration in *tat1*$^{-/-}$ as in *wt*. The organ concentrations of all non-AAAs were similar in *tat1*$^{-/-}$ as in *wt* animals, as shown for L-Val and L-Leu (Fig. 4). One peculiarity is the high L-Phe values measured in kidney. This value might be related to the role of the kidney for the production of L-Tyr from L-Phe.

Altered epithelial AA transport

The analysis of 24 h urine collected in metabolic cages showed that the dietary switch did not affect the AA excretion in *wt* animals (Fig. 5*A*). *tat1*$^{-/-}$ mice presented an aromatic aminoaciduria under normal protein diet that paralleled the high plasma values (Fig. 5*B*). However, under high protein diet, L-Tyr was found to be 64 times more abundant in *tat1*$^{-/-}$ than in *wt* urine, and L-Trp and L-Phe, 95 and 9 times, respectively. Furthermore, many other neutral AAs were also present in higher amounts in *tat1*$^{-/-}$ urine (i.e. between two- and ninefold), including all other substrates of the Lat2–4F2hc broad selectivity neutral AA exchanger. This indicates that under normal protein diet *tat1*$^{-/-}$ mice had an almost normal or only slightly increased fractional excretion of all AAs. In contrast, the high protein diet provoked in *tat1*$^{-/-}$ mice a high urinary excretion of AAs corresponding to a major increase of their fractional excretion. This inability of the kidney to maintain a low fractional excretion was selective of AAs, as all other measured urinary parameters did not display any significant difference between *tat1*$^{-/-}$ and *wt* control mice (Table 1).

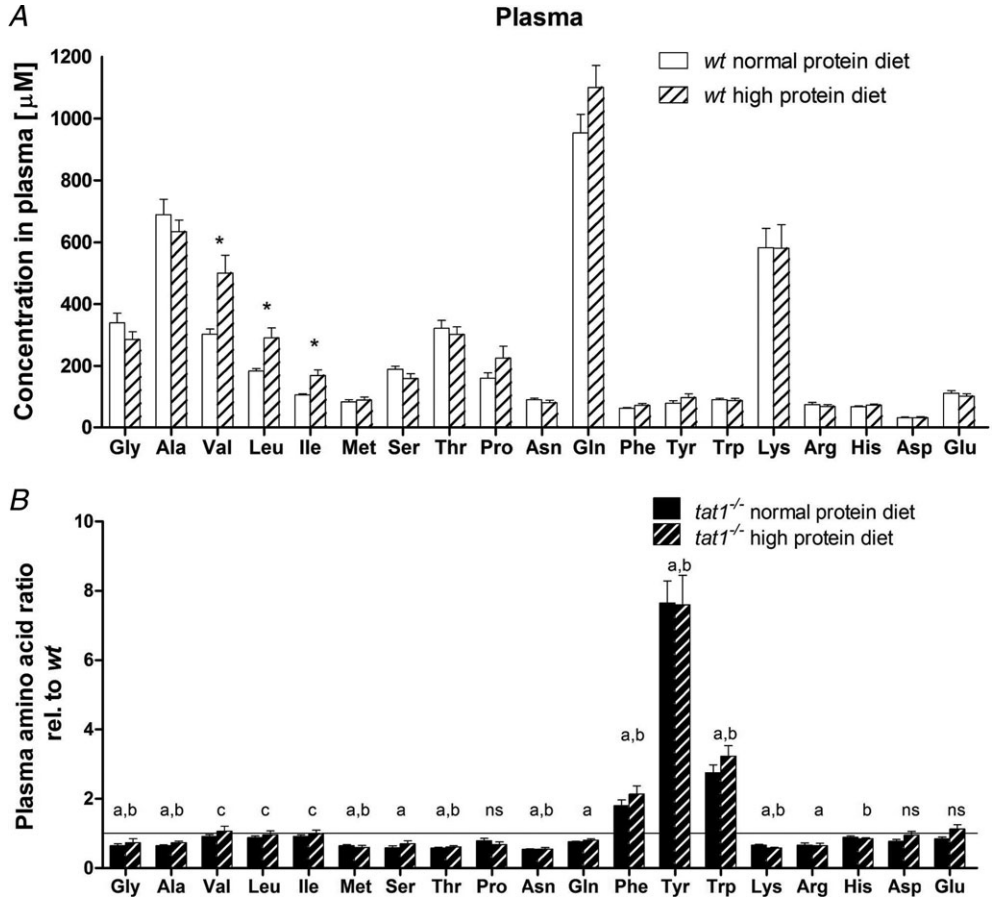

Figure 3. Free circulating AAs in plasma: effect of high protein diet in *wt* mice (*A*) and altered AA profile in *tat1*$^{-/-}$ (*B*)

A, absolute concentrations of AAs measured in plasma of *wt* mice subjected to normal (20%) and high (40%) protein diet. *$P < 0.05$. *B*, plasma AA concentrations in *tat1* knockout mice are shown relative to the values measured for their *wt* littermates under the same diet. The horizontal line ($y = 1$) corresponds to the *wt* values. Represented are means ± SEM ($n = 12$). Groups were compared by one-way ANOVA, followed by Bonferroni *post hoc* test on selected pairs of columns. Values with letters are statistically different ($P < 0.05$): 'a' and 'b' indicate difference of *tat1*$^{-/-}$ *versus wt* under normal protein diet and high protein diet, respectively; 'c' indicates difference between normal protein and high protein diet in *tat1*$^{-/-}$ mice; ns, all comparison are not significant.

Because TAT1 is expressed in the basolateral but not in the apical membrane of kidney proximal tubule, we hypothesize that the observed aminoaciduria might derive from an impaired basolateral export rather than from a defective apical import into epithelial cells. To verify this hypothesis, we used the isotopes ^{123}I-2-I-L-Phe and ^{125}I-2-I-L-Phe. These iodinated AAs are used as markers for oncologic imaging outside the brain, as their accumulation reflects the increased AA transport activity of cancer cells (Jager *et al.* 2001; Lahoutte *et al.* 2003). Their biodistribution has already been assessed and their validity demonstrated (Lahoutte *et al.* 2001, 2003, 2004). When tested in the *Xenopus laevis* oocytes expression system, the compound (2-I-L-Phe) was shown to efficiently compete for L-Phe transport, whether mediated by TAT1, Lat4 (Slc43a2) or Lat2–4F2hc (Supplemental Fig. 5). Exploiting the micro-SPECT/CT technique, the ^{123}I-2-I-L-Phe isotope was used for live imaging of its distribution 30 min after intravenous injection (Fig. 6). Indeed a higher accumulation of the compound was clearly detected in both kidneys of the *tat1*$^{-/-}$ mouse (Fig. 6*B*). This qualitative observation was verified by the quantification of the accumulated counts after death ($n = 3$; Fig. 6*C*).

Like the kidney proximal tubule, TAT1 is also expressed in the basolateral membrane of epithelial cells along the small intestine (Ramadan *et al.* 2006; Supplemental Table 1). Therefore, AA transport was measured in everted gut sacs. A significant accumulation of L-[^{3}H]Phe was observed in the enterocytes after 10 min incubation at 37°C (Fig. 7). Also a tendency for decreased net transepithelial transport into the serosal compartment was observed. These data support the hypothesis that TAT1 absence reduces the transepithelial transport of AAAs by decreasing their basolateral efflux.

Discussion

Although the lack of TAT1 does not prevent the normal development and fertility of mice, the study of the newly developed *tat1*$^{-/-}$ mouse revealed a number of important functions of this low-affinity AAA uniporter that impact on body AA homeostasis. For instance, the disruption of TAT1 is shown to prevent the liver in playing its central role for the metabolism of AAAs. It is indeed well known that the accumulation of AAs as response to high protein diet is counteracted by an increase in liver AA catabolism (Moundras *et al.* 1993). In particular, the liver is the major metabolic organ for the catabolism of AAAs (Schimassek & Gerok, 1965; Brosnan, 2003), and its failure causes an increase of AAAs in plasma (Fischer *et al.* 1976; Brosnan, 2003). This leads to a decrease of the BCAAs/AAAs ratio (Fischer ratio), and the consecutive increase of AAA uptake into the brain has been suggested to be a major cause of hepatic encephalopathy (James *et al.* 1979; Dejong *et al.* 2007). Here we show that plasma AAAs are stably elevated in *tat1*$^{-/-}$ mice regardless of the dietary load (Fig. 3). This increase is reflected in skeletal muscles, suggesting that TAT1 is not necessary for the AAA equilibration between plasma and this compartment (Fig. 4; Supplemental Table 1b). In contrast, in the liver of *tat1*$^{-/-}$ mice the intracellular AAA values are normal, indicating that the transport between the plasma that contains an elevated AAA concentration and this organ is uncoupled (Fig. 8). The present data document that

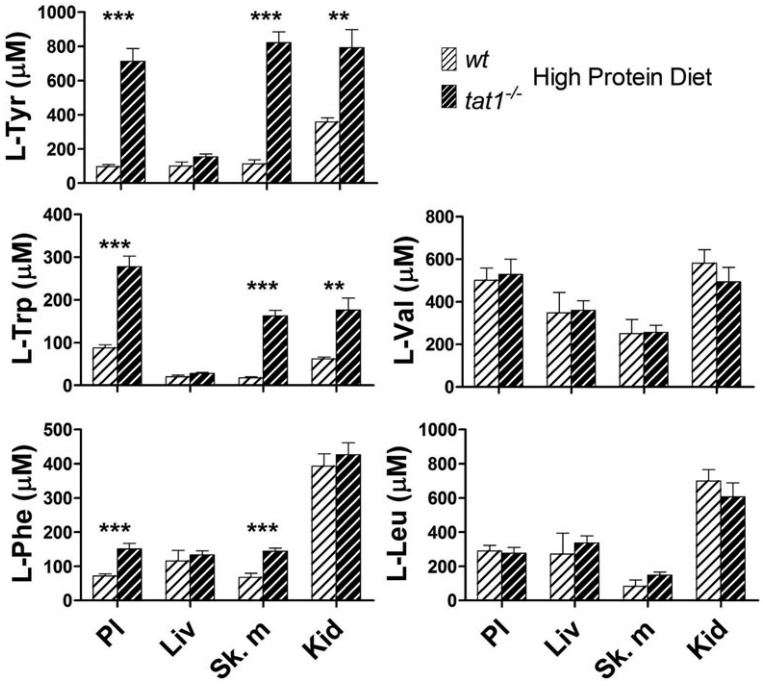

Figure 4. Concentrations of free AAs in plasma and cytosol of different organs
PL, plasma; Liv, liver; Sk. m, skeletal muscles (i.e. m. gastrocnemius); Kid, kidney. Represented are means ± SEM ($n = 6$). $^{**}P < 0.01$; $^{***}P < 0.001$ by unpaired Student's *t* test. More AAs can be found in Supplemental Fig. 6.

tat1 mediates the equilibration of the extracellular AAA concentration with the hepatocytes, and suggests that the liver functions as a sink for the AAAs and thereby sets their concentration and controls their body homeostasis.

AAAs play important roles in the brain. Both increased and decreased levels are thought to impair brain function, as mentioned above for the increase in AAAs due to liver failure that contributes to hepatic encephalopathy. Dietary L-Trp restriction that was shown in mice to result in altered emotional response to stress and increased locomotor activity is one example in which a decreased level of AAAs leads to an alteration of brain functions (Uchida *et al.* 2005). However, a more recent study found no correlation between L-Trp depletion, central serotonin reduction and affective behavioural changes (van Donkelaar *et al.* 2010). The lack of signs of hepatic encephalopathy or behavioural disorders in *tat1*$^{-/-}$ suggests that the AAA concentration within the brain is normal or at a level that has no gross functional consequences. This suggests that the blood–brain barrier function is intact, as expected based on our observation that *tat1* is not expressed in mouse blood–brain barrier endothelial cells (Lyck *et al.* 2009).

The absence of behavioural and growth alterations also suggests that the lack of TAT1 does not have a major impact on the function of thyroid hormone, although this transporter was shown to facilitate the diffusion of both T3 and T4 (Friesema *et al.* 2008). Recent investigations from the laboratory of Heike Heuer indeed confirm that thyroid hormone metabolism is not altered in TAT1 null mice (personal communication).

The placenta is another cellular barrier that expresses TAT1 but for which this transporter appears to be dispensable in laboratory conditions (Meredith & Christian, 2008). Indeed, *tat1*$^{-/-}$ foetus develops normally

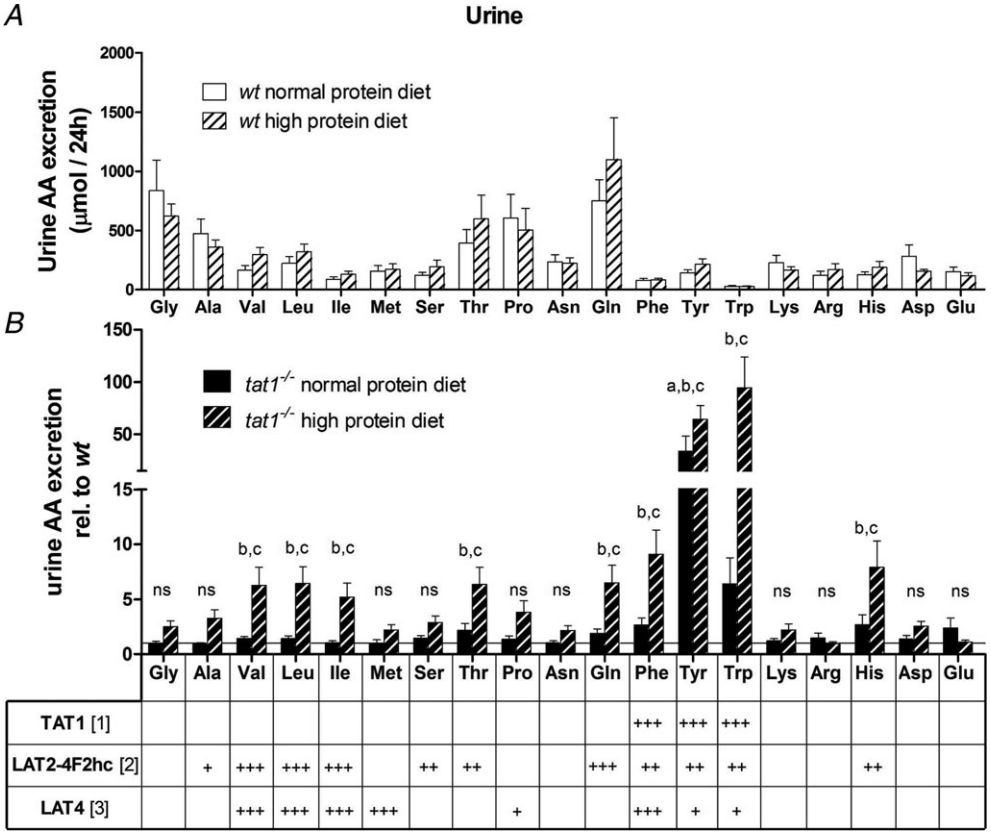

Figure 5. Urinary amino acid (AA) profiles: the high protein diet has no effect on *wt* mice (*A*) but enhances the aminoaciduria in *tat1*$^{-/-}$ (*B*)

A, total AAs excreted in 24 h by *wt* mice subjected to normal (20%) and high (40%) protein diet. *B*, AAs excreted in *tat1* knockout mice are shown relative to the values measured for their *wt* littermates under the same diet. The horizontal line ($y = 1$) corresponds to normalized *wt* values. The selectivity of known basolateral AA transporters measured in *Xenopus laevis* oocyte expression system is indicated below (References: [1] corresponds to Ramadan *et al.* 2007; [2] to Meier *et al.* 2002; Park *et al.* 2005; and [3] to Bodoy *et al.* 2005). +++ indicates high, ++ intermediate, + low, and empty space no selectivity. Represented are means ± SEM ($n = 12$). Groups were compared by one-way ANOVA, followed by Bonferroni *post hoc* test on selected pairs of columns. Values with letters are statistically different ($P < 0.05$): 'a' *tat1*$^{-/-}$ *versus wt* in NPD, 'b' *tat1*$^{-/-}$ *versus wt* in HPD, 'c' *tat1*$^{-/-}$ NPD *versus* HPD, 'd' *wt* NPD *versus* HPD, 'ns' all comparisons are not significant.

and *tat1*$^{-/-}$ female mice are normally fertile. After birth, *tat1*$^{-/-}$ mice maintain the capacity to absorb AAs from nutritional sources. This indicates that intestinal AA absorption and in particular the basolateral efflux of (aromatic) AAs from enterocytes is possible also in the absence of TAT1. We therefore tested for the upregulation of some other transporters that could compensate for the lack of TAT1. However, none of the other basolateral neutral AA transporters was found to be upregulated at the mRNA level in intestine and kidney, which suggested that the residual AAA transport capacity and potential paracellular transport can compensate for *tat1* absence under normal diet.

An important finding is the massive loss of AAAs and more discrete loss of all substrate AAs of the neutral exchanger Lat2–4F2hc in the urine of *tat1*$^{-/-}$ mice under high protein diet (Fig. 5). This aminoaciduria implies that the maximal transport capacity for these AAs was exceeded in kidney proximal tubule, and reveals the role of TAT1 for epithelial AA transport. Furthermore, it is suggested that this (aromatic) AA loss explains the fact that the *tat1*$^{-/-}$ mouse plasma AA concentration does not additionally change much under high protein diet. In our assay the urine was collected over 24 h, whereas the blood was collected once (i.e. 3 h after the switch to the inactive light phase). It is thus conceivable that under normal protein diet the AA transport rate is near the maximal transport capacity of the proximal tubule, already within the so-called splay, where some nephrons do not have the capacity of reabsorbing all substrates. Because the plasma AA levels depend also on nutritional intake and are higher during the absorptive phase, under high protein diet a transient increase in blood AAs might cause the AA spillover. The urinary AA pattern (very high TAT1 substrates, increased Lat2–4F2hc substrates) is in line with the suggested functional cooperation of the uniporter TAT1 with the exchanger Lat2–4F2hc for the net efflux of neutral AAs, as previously shown in the *Xenopus laevis* expression system (Ramadan *et al.* 2007). Interestingly, the loss of L-Phe in the urine was lower than that of L-Tyr and L-Trp. We hypothesize that this is due to the ability of another basolateral uniporter to transport L-Phe. Indeed, we have shown that Lat4 (Slc43a2) is also localized in the basolateral membrane of proximal kidney tubule cells and of small intestine enterocytes (Bodoy *et al.* 2005; L. Mariotta, A. Guetg & F. Verrey, unpublished data). This transporter was first described by Bodoy *et al.* in 2005 and shown to mediate the facilitated diffusion of BCAAs, L-Met and

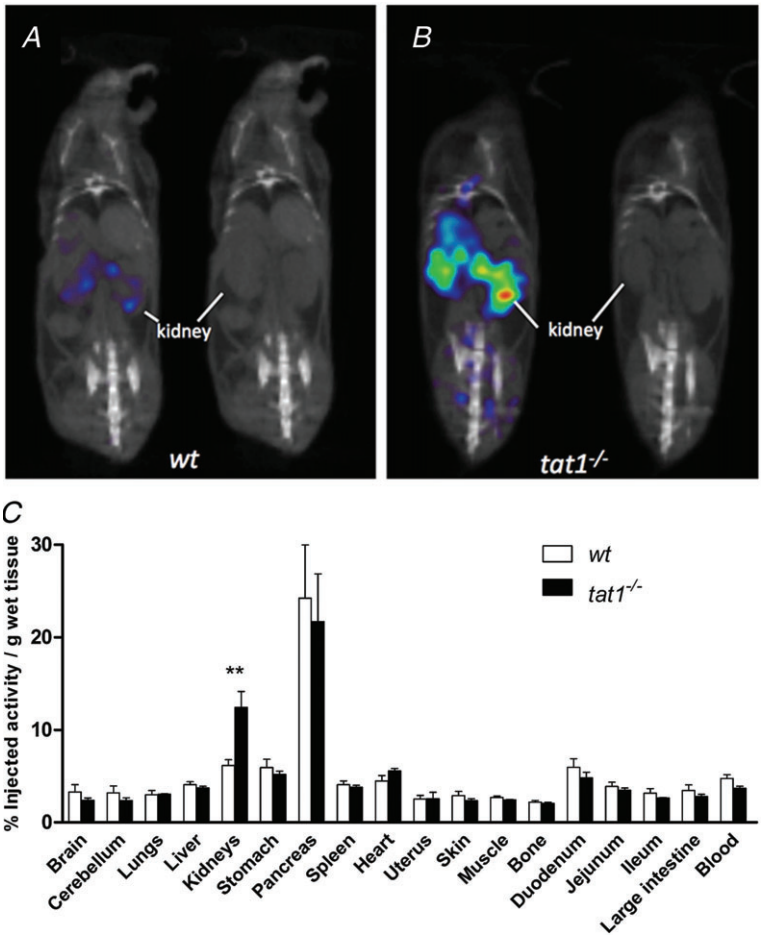

Figure 6. ^{123}I-2-I-L-Phe accumulation in kidney after I.V. injection
Fused micro-SPECT/CT and micro-CT coronal scans of a *wt* (*A*) and a *tat1*$^{-/-}$ (*B*) mouse: the *tat1*$^{-/-}$ animal presented a clear accumulation of the compound in both kidneys, whereas kidney accumulation was low in *wt*. *C*, quantification of the biodistribution in different organs after dissection. Represented is the percentage of injected activity of ^{123}I-2-I-L-Phe in each tissue or organ per gram. Given are means ± SEM ($n = 3$). $^{**}P < 0.01$ by unpaired Student's *t* test.

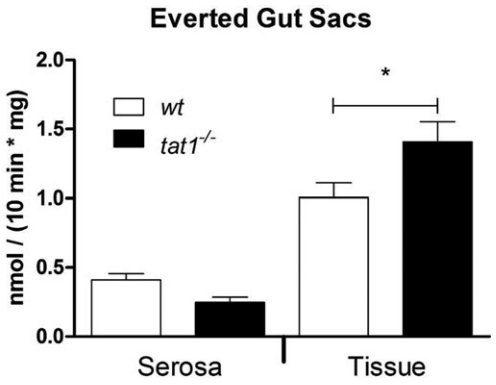

Figure 7. Significant accumulation of L-Phe in intestinal everted gut sacs
Everted sacs of *tat1*$^{-/-}$ and *wt* mouse small intestine were incubated at 37°C for 10 min in Krebs buffer containing 100 μM L-Phe and L-[^{3}H]Phe tracer. Radioactivity was counted inside of the sacs (serosa) and in the tissue (epithelial cells). Transport rates were calculated and normalized to weight of tissue. Represented are means ± SEM ($n \geq 8$). *$P < 0.05$ by unpaired Student's *t* test.

L-Phe and, to a lesser extent, L-Pro, L-Tyr and L-Trp. The presence of this other uniporter for essential AAs and its selectivity might explain the differential urinary AAA pattern observed in *tat1*$^{-/-}$ mice (ninefold more L-Phe *versus* 64- and 95-fold more L-Tyr and L-Trp, respectively). Furthermore, Lat4 could to a large extent compensate for the absence of TAT1 in kidney and intestine, and thus explain the mild phenotype of *tat1*$^{-/-}$ mice. The lack of Lat4 expression in the liver does on the other hand explain the fact that in the absence of *tat1* expression, the liver cannot function as a sink for AAAs (Bodoy *et al.* 2005).

To verify that AAAs are efficiently imported luminally into transporting epithelial cells of *tat1*$^{-/-}$ mice, where they accumulate due to their inefficient basolateral export and consequently inhibit the apical transport, *in vivo* micro-SPECT/CT and *ex vivo* everted gut sac experiments were performed. The results confirmed the accumulation of tracers inside the epithelial cells (Figs 6 and 7). However, the everted gut sacs experiments did not allow us to detect a significant difference in the net transcellular flux of L-Phe (Fig. 7: serosa). This was due to a substantial residual permeability of the small intestine epithelium of *tat1*$^{-/-}$ mice for AAAs that might explain the normal growth of *tat1*$^{-/-}$ mice. This residual permeability is presumably due to a large extent to the contribution of the other uniporter Lat4, as mentioned above. We hypothesize, however, that a paracellular leak might also contribute to this permeability, as previously suggested for glucose and phosphate (Danisi & Murer, 1991; Pappenheimer, 1993; Ballard *et al.* 1995).

A defect in *tat1* has been predicted to be the cause of the blue diaper syndrome (Kim *et al.* 2001; Broer, 2008; Broer & Palacin, 2011). This syndrome was initially described by Drummond and co-workers in 1964, and appears to be caused by an excess of unabsorbed L-Trp in the intestinal tract (Drummond *et al.* 1964). We did not observe any symptom reminiscent of this syndrome in *tat1*$^{-/-}$ mice. Furthermore, the amount of L-Trp found in the distal part of the small intestine was similar to *wt* (Supplemental Fig. 6) and much less than observed in Hartnup disorder (D. Singer & F. Verrey, unpublished results).

In summary, the analysis of *tat1*$^{-/-}$ mice confirmed that a complex machinery of AA transporters functionally

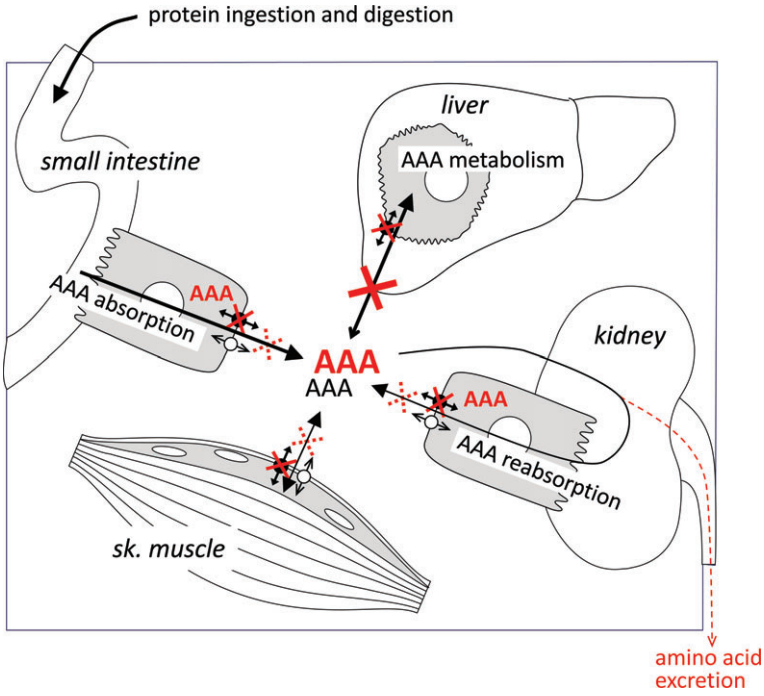

Figure 8. Schematic representation of the impact of TAT1 deletion on body aromatic amino acid (AAA) homeostasis
Black arrows indicate AAA transport across cell membranes in the presence of TAT1 (black uniporter symbol). The red crosses and AAA labels indicate the situation in *tat1*$^{-/-}$ mice. The lack of TAT1-mediated AAAs diffusion into liver hepatocytes (major site of AAA metabolism) leads to a higher steady state AAA level in plasma. In the absence of TAT1, the transport of AAA is also decreased at the basolateral membrane of small intestine enterocytes and kidney proximal tubule cells, and in skeletal muscle cells. However, AAA transport is maintained across these membranes via (an) additional transporter(s) (empty uniporter symbol). Nonetheless, accumulation of AAAs was observed in these epithelial cells (indicated as red AAA).

cooperates for the absorption and distribution of dietary AAs (Fig. 8). Our data further indicate that TAT1 exerts a major homeostatic function by equilibrating the concentration of AAAs between plasma and hepatocytes, where the AAAs are in turn catabolized. The functional impact of TAT1 absence becomes more evident under high protein diet, when the transport capacity of the kidney is exceeded such that a massive aromatic and also a neutral aminoaciduria appear that contributes in maintaining AA plasma homeostasis. We show that the aminoaciduria originates from an accumulation of AAs in the epithelial cells and we postulate that another basolateral uniporter, Lat4 (Slc43a2), compensates to a substantial extent for the lack of TAT1, in particular for driving the export function of the exchangers Lat2–4F2hc and y^+Lat1–4F2hc in small intestine and kidney proximal tubule.

References

Augustin M, Sedlmeier R, Peters T, Huffstadt U, Kochmann E, Simon D, Schoniger M, Garke-Mayerthaler S, Laufs J, Mayhaus M, Franke S, Klose M, Graupner A, Kurzmann M, Zinser C, Wolf A, Voelkel M, Kellner M, Kilian M, Seelig S, Koppius A, Teubner A, Korthaus D, Nehls M & Wattler S (2005). Efficient and fast targeted production of murine models based on ENU mutagenesis. *Mamm Genome* **16**, 405–413.

Ballard ST, Hunter JH & Taylor AE (1995). Regulation of tight-junction permeability during nutrient absorption across the intestinal epithelium. *Annu Rev Nutr* **15**, 35–55.

Bauwens M, Lahoutte T, Kersemans K, Caveliers V, Bossuyt A & Mertens J (2007). D- and L-[123I]-2-I-phenylalanine show a long tumour retention compared with D- and L-[123I]-2-I-tyrosine in R1M rhabdomyosarcoma tumour-bearing Wag/Rij rats. *Contrast Media Mol Imaging* **2**, 172–177.

Bodoy S, Martin L, Zorzano A, Palacin M, Estevez R & Bertran J (2005). Identification of LAT4, a novel amino acid transporter with system L activity. *J Biol Chem* **280**, 12002–12011.

Braun D, Wirth EK, Wohlgemuth F, Reix N, Klein MO, Gruters A, Kohrle J & Schweizer U (2011). Aminoaciduria, but normal thyroid hormone levels and signalling, in mice lacking the amino acid and thyroid hormone transporter Slc7a8. *Biochem J* **439**, 249–255.

Broer S (2008). Apical transporters for neutral amino acids: physiology and pathophysiology. *Physiology (Bethesda)* **23**, 95–103.

Broer S & Palacin M (2011). The role of amino acid transporters in inherited and acquired diseases. *Biochem J* **436**, 193–211.

Brosnan JT (2003). Interorgan amino acid transport and its regulation. *J Nutr* **133**, 2068S–2072S.

Cynober LA (2002). Plasma amino acid levels with a note on membrane transport: characteristics, regulation, and metabolic significance. *Nutrition* **18**, 761–766.

Danisi G & Murer H (1991). Inorganic phosphate absorption in small intestine. In *Comprehensive Physiology*, Supplement 19: Handbook of Physiology, The Gastrointestinal System, Intestinal Absorption and Secretion: 323–336.

Dejong CH, van de Poll MC, Soeters PB, Jalan R & Olde Damink SW (2007). Aromatic amino acid metabolism during liver failure. *J Nutr* **137**, 1579S–1585S; discussion 1597S–1598S.

Drummond KN, Michael AF, Ulstrom RA & Good RA (1964). The blue diaper syndrome: familial hypercalcemia with nephrocalcinosis and indicanuria; a new familial disease, with definition of the metabolic abnormality. *Am J Med* **37**, 928–948.

Fernandez E, Torrents D, Chillaron J, Martin Del Rio R, Zorzano A & Palacin M (2003). Basolateral LAT-2 has a major role in the transepithelial flux of L-cystine in the renal proximal tubule cell line OK. *J Am Soc Nephrol* **14**, 837–847.

Fischer JE, Rosen HM, Ebeid AM, James JH, Keane JM & Soeters PB (1976). The effect of normalization of plasma amino acids on hepatic encephalopathy in man. *Surgery* **80**, 77–91.

Friesema EC, Jansen J, Jachtenberg JW, Visser WE, Kester MH & Visser TJ (2008). Effective cellular uptake and efflux of thyroid hormone by human monocarboxylate transporter 10. *Mol Endocrinol* **22**, 1357–1369.

Jager PL, Vaalburg W, Pruim J, de Vries EG, Langen KJ & Piers DA (2001). Radiolabeled amino acids: basic aspects and clinical applications in oncology. *J Nucl Med* **42**, 432–445.

James JH, Ziparo V, Jeppsson B & Fischer JE (1979). Hyperammonaemia, plasma aminoacid imbalance, and blood-brain aminoacid transport: a unified theory of portal-systemic encephalopathy. *Lancet* **2**, 772–775.

Karl T, Pabst R & von Horsten S (2003). Behavioral phenotyping of mice in pharmacological and toxicological research. *Exp Toxicol Pathol* **55**, 69–83.

Keays DA, Clark TG, Campbell TG, Broxholme J & Valdar W (2007). Estimating the number of coding mutations in genotypic and phenotypic driven N-ethyl-N-nitrosourea (ENU) screens: revisited. *Mamm Genome* **18**, 123–124.

Kim DK, Kanai Y, Chairoungdua A, Matsuo H, Cha SH & Endou H (2001). Expression cloning of a Na^+-independent aromatic amino acid transporter with structural similarity to H^+/monocarboxylate transporters. *J Biol Chem* **276**, 17221–17228.

Lahoutte T, Caveliers V, Camargo SM, Franca R, Ramadan T, Veljkovic E, Mertens J, Bossuyt A & Verrey F (2004). SPECT and PET amino acid tracer influx via system L (h4F2hc-hLAT1) and its transstimulation. *J Nucl Med* **45**, 1591–1596.

Lahoutte T, Caveliers V, Dierickx L, Vekeman M, Everaert H, Mertens J & Bossuyt A (2001). *In vitro* characterization of the influx of 3-[^{125}I]iodo-L-alpha-methyltyrosine and 2-[^{125}I]iodo-L-tyrosine into U266 human myeloma cells: evidence for system T transport. *Nucl Med Biol* **28**, 129–134.

Lahoutte T, Caveliers V, Franken PR, Bossuyt A, Mertens J & Everaert H (2002). Increased tumor uptake of 3-$^{(123)}$I-Iodo-L-alpha-methyltyrosine after preloading with amino acids: an *in vivo* animal imaging study. *J Nucl Med* **43**, 1201–1206.

Lahoutte T, Mertens J, Caveliers V, Franken PR, Everaert H & Bossuyt A (2003). Comparative biodistribution of iodinated amino acids in rats: selection of the optimal analog for

oncologic imaging outside the brain. *J Nucl Med* **44**, 1489–1494.
Loening AM & Gambhir SS (2003). AMIDE: a free software tool for multimodality medical image analysis. *Mol Imaging* **2**, 131–137.
Lyck R, Ruderisch N, Moll AG, Steiner O, Cohen CD, Engelhardt B, Makrides V & Verrey F (2009). Culture-induced changes in blood-brain barrier transcriptome: implications for amino-acid transporters *in vivo*. *J Cereb Blood Flow Metab* **29**, 1491–1502.
Maquat LE (1995). When cells stop making sense: effects of nonsense codons on RNA metabolism in vertebrate cells. *RNA* **1**, 453–465.
Meier C, Ristic Z, Klauser S & Verrey F (2002). Activation of system L heterodimeric amino acid exchangers by intracellular substrates. *EMBO J* **21**, 580–589.
Meredith D & Christian HC (2008). The SLC16 monocarboxylate transporter family. *Xenobiotica* **38**, 1072–1106.
Moundras C, Remesy C & Demigne C (1993). Dietary protein paradox: decrease of amino acid availability induced by high-protein diets. *Am J Physiol Gastrointest Liver Physiol* **264**, G1057–G1065.
Nassl AM, Rubio-Aliaga I, Fenselau H, Marth MK, Kottra G & Daniel H (2011). Amino acid absorption and homeostasis in mice lacking the intestinal peptide transporter PEPT1. *Am J Physiol Gastrointest Liver Physiol* **301**, G128–G137.
Pappenheimer JR (1993). On the coupling of membrane digestion with intestinal absorption of sugars and amino acids. *Am J Physiol Gastrointest Liver Physiol* **265**, G409–G417.
Park SY, Kim JK, Kim IJ, Choi BK, Jung KY, Lee S, Park KJ, Chairoungdua A, Kanai Y, Endou H & Kim DK (2005). Reabsorption of neutral amino acids mediated by amino acid transporter LAT2 and TAT1 in the basolateral membrane of proximal tubule. *Arch Pharm Res* **28**, 421–432.
Pfeiffer R, Rossier G, Spindler B, Meier C, Kuhn L & Verrey F (1999). Amino acid transport of y+L-type by heterodimers of 4F2hc/CD98 and members of the glycoprotein-associated amino acid transporter family. *EMBO J* **18**, 49–57.
Ramadan T, Camargo SM, Herzog B, Bordin M, Pos KM & Verrey F (2007). Recycling of aromatic amino acids via TAT1 allows efflux of neutral amino acids via LAT2–4F2hc exchanger. *Pflugers Arch* **454**, 507–516.
Ramadan T, Camargo SM, Summa V, Hunziker P, Chesnov S, Pos KM & Verrey F (2006). Basolateral aromatic amino acid transporter TAT1 (Slc16a10) functions as an efflux pathway. *J Cell Physiol* **206**, 771–779.
Rossier G, Meier C, Bauch C, Summa V, Sordat B, Verrey F & Kuhn LC (1999). LAT2, a new basolateral 4F2hc/CD98-associated amino acid transporter of kidney and intestine. *J Biol Chem* **274**, 34948–34954.
Schimassek H & Gerok W (1965). Control of the levels of free amino acids in plasma by the liver. *Biochem Z* **343**, 407–415.
Seaton B & Ali A (1984). Simplified manual high performance clinical chemistry methods for developing countries. *Med Lab Sci* **41**, 327–336.
Sugiura S, Kitagawa K, Tanaka S, Todo K, Omura-Matsuoka E, Sasaki T, Mabuchi T, Matsushita K, Yagita Y & Hori M (2005). Adenovirus-mediated gene transfer of heparin-binding epidermal growth factor-like growth factor enhances neurogenesis and angiogenesis after focal cerebral ischemia in rats. *Stroke* **36**, 859–864.
Uchida S, Kitamoto A, Umeeda H, Nakagawa N, Masushige S & Kida S (2005). Chronic reduction in dietary tryptophan leads to changes in the emotional response to stress in mice. *J Nutr Sci Vitaminol* **51**, 175–181.
van Donkelaar EL, Blokland A, Lieben CK, Kenis G, Ferrington L, Kelly PA, Steinbusch HW & Prickaerts J (2010). Acute tryptophan depletion in C57BL/6 mice does not induce central serotonin reduction or affective behavioural changes. *Neurochem Int* **56**, 21–34.
Vanhove C, Defrise M, Bossuyt A & Lahoutte T (2011). Improved quantification in multiple-pinhole SPECT by anatomy-based reconstruction using microCT information. *Eur J Nucl Med Mol Imaging* **38**, 153–165.
Verrey F (2003). System L: heteromeric exchangers of large, neutral amino acids involved in directional transport. *Pflugers Arch* **445**, 529–533.
Verrey F, Singer D, Ramadan T, Vuille-dit-Bille RN, Mariotta L & Camargo SM (2009). Kidney amino acid transport. *Pflugers Arch* **458**, 53–60.
Wu G (2009). Amino acids: metabolism, functions, and nutrition. *Amino Acids* **37**, 1–17.
Wybenga DR, Di Giorgio J & Pileggi VJ (1971). Manual and automated methods for urea nitrogen measurement in whole serum. *Clin Chem* **17**, 891–895.

Author contributions

L.M., S.M.R.C., T.L. and F.V.: conception and design of the experiment. L.M., D.S., A.G., B.H., S.M.R.C. and F.V.: collection, analysis and interpretation of data. L.M. and F.V.: drafting and revising the article. All authors approved the final version.

Acknowledgements

The authors thank David Wolfer for his help in using the RotaRod, Hannelore Daniel for helpful discussions, and the Functional Genomics Center Zurich (FGCZ) for the amino acid analysis. This work was supported by the Swiss National Science Foundation grant 31-130471 to F.V.